

Supporting Information

Multi-stimuli Responsive Behavior of Two Zn(II) Complexes Based on a Schiff Base with High Contrast

Zhong-Gang Xia^a, Yong-Sheng Shi^a, Tong Xiao^a and Xiang-Jun Zheng^{a*}

^a *Beijing Key Laboratory of Energy Conversion and Storage Materials, College of Chemistry, Beijing Normal University, Beijing 100875, P. R. China.*

Corresponding author:

Tel.: +86-10-58805522; fax: +86-10-58802075.

E-mail address: xjzheng@bnu.edu.cn (X. -J. Zheng)

Contents

Materials and instrumentation

Figure S1. Fluorescence excitation and emission spectra of **1** (a) and **2** (b).

Figure S2. Fluorescence decay curves and fit results of complexes **1** (a) and **2** (b).

Figure S3. (a) Photographs under ambient light and 365 nm UV light. (b) PXRD patterns. (c) Fluorescence emission spectra of complex **2** and the samples exposed to HCl/NH₃ vapor. (d) IR spectra of complex **2** exposed to NH₃ vapor.

Figure S4. Fluorescence emission spectra of **B**, **1-NH₃** and **2-NH₃**.

Figure S5. (a) Photographs under ambient light and 365 nm UV light. (b) PXRD patterns. (c) Fluorescence emission spectra of complex **2** and the samples exposed to HCl/NH₃ vapor.

Figure S6. Thermogravimetric curves of complex **1** (a) and complex **2** (b) before and after fumigation by HCl vapor.

Comparison of the fluorescence of complex **1** and the Schiff base ligand

Figure S7 The optimized molecular configurations and orbitals (HOMO and LUMO) of complex **1** and Schiff base ligand.

Figure S8 Molecular structure of complex **1** (a) and Schiff base ligand (b) showing the distortion angle between the pyridine and benzene planes.

Figure S9. IR spectra of **1-HCl-NH₃** and **2-HCl-NH₃**.

Figure S10. UV-vis absorption spectra of complexes **1** (a) and **2** (b) before and after grinding and fumed.

Figure S11. (a) Photographs under ambient light and 365 nm UV light. (b) PXRD patterns. (c) Fluorescence emission spectra of the original crystals of complex **2** before and after grinding and fumed.

Figure S12. Thermogravimetric curves of complex **1** (a) and complex **2** (b) after grinding.

Figure S13. Photographs of the complex **2** test paper after different treatments under natural light and 365 nm irradiation.

Table S1 Crystal data and structure refinement parameters of complexes **1** and **2**.

Table S2. Selected bond distances (Å) and angles (°) for **1** and **2**.

Table S3. The photophysical data of complex **1** in different states.

Table S4. The photophysical data of complex **2** in different states.

Table S5. The fluorescence lifetime $\langle\tau\rangle$ of **1** and **2**.

Materials and instrumentation

All solvents and reagents (analytical grade and spectroscopic grade) were used as received. Single crystal X-ray diffraction data were collected by XtaLAB Synergy-DW area-detector diffractometer using mirror optics monochromated Cu-K α radiation ($\lambda = 1.54184 \text{ \AA}$) at low temperature (100 K). Fourier transform infrared (FT-IR) spectra were recorded on an Avatar 360 FT-IR spectrometer using KBr pellets in 4000-400 cm^{-1} . X-ray powder diffraction (PXRD) pattern was collected using a SHIMADZU XRD-7000 diffractometer with Cu K α radiation ($\lambda = 1.5418 \text{ \AA}$) at 25°C. Elemental analyses (CHN) were conducted using a Vario EL elemental analyzer. Thermogravimetric data (TGA) were obtained using a Mettler TGA instrument in the range of 25–500°C under nitrogen flow with a heating rate of 10°C min^{-1} . The fluorescence spectra were recorded on an FLS980 fluorescence spectrophotometer with a quartz cuvette (path length of 1 cm). Solid-state UV–Vis absorption spectra were recorded on a TU-1901 spectrophotometer with an integrating sphere at room temperature in the range of 250–800 nm.

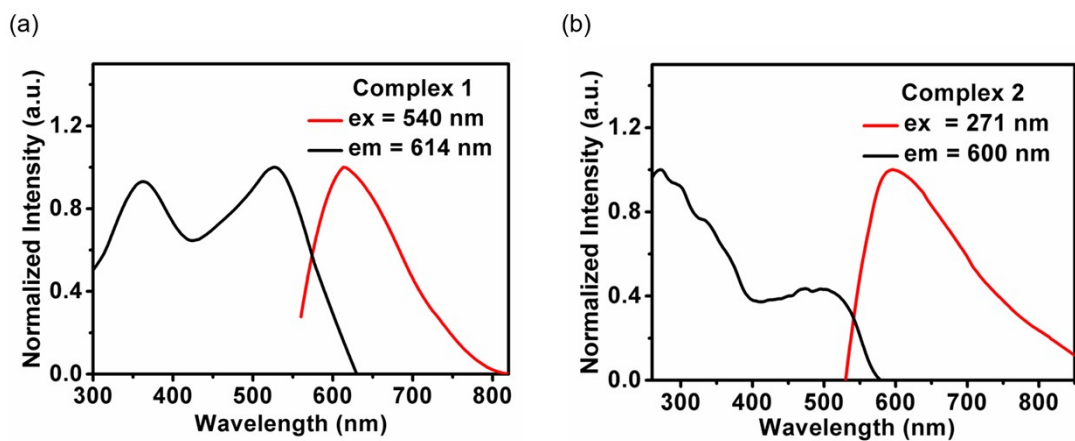


Figure S1. Fluorescence excitation and emission spectra of **1** (a) and **2** (b).

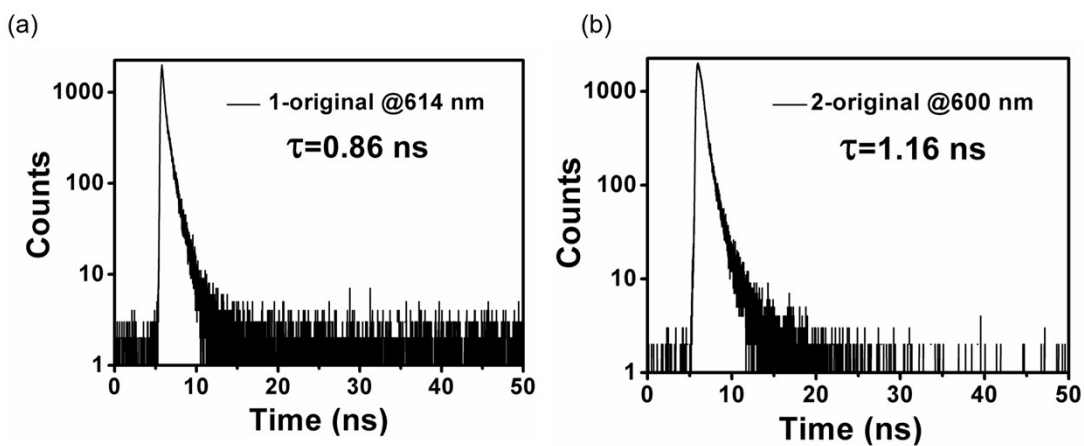


Figure S2. Fluorescence decay curves and fit results of complexes **1** (a) and **2** (b).

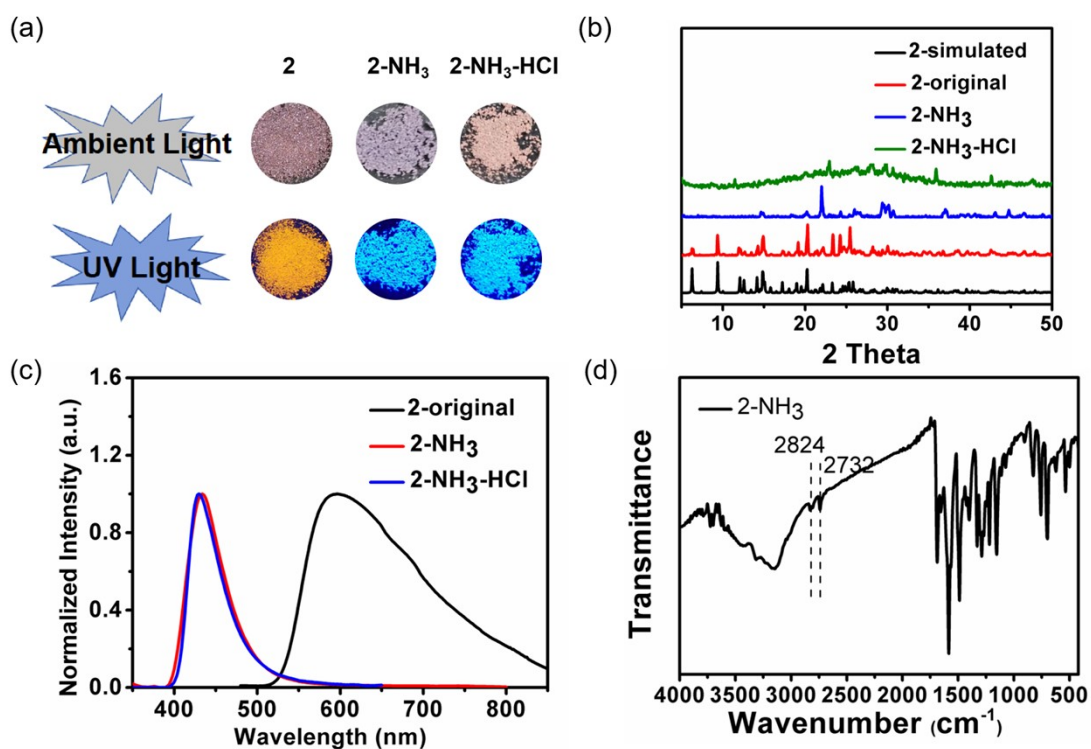


Figure S3. (a) Photographs under ambient light and 365 nm UV light. (b) PXRD patterns. (c) Fluorescence emission spectra of complex **2** and the samples exposed to HCl/NH₃ vapor. (d) IR spectra of complex **2** exposed to NH₃ vapor.

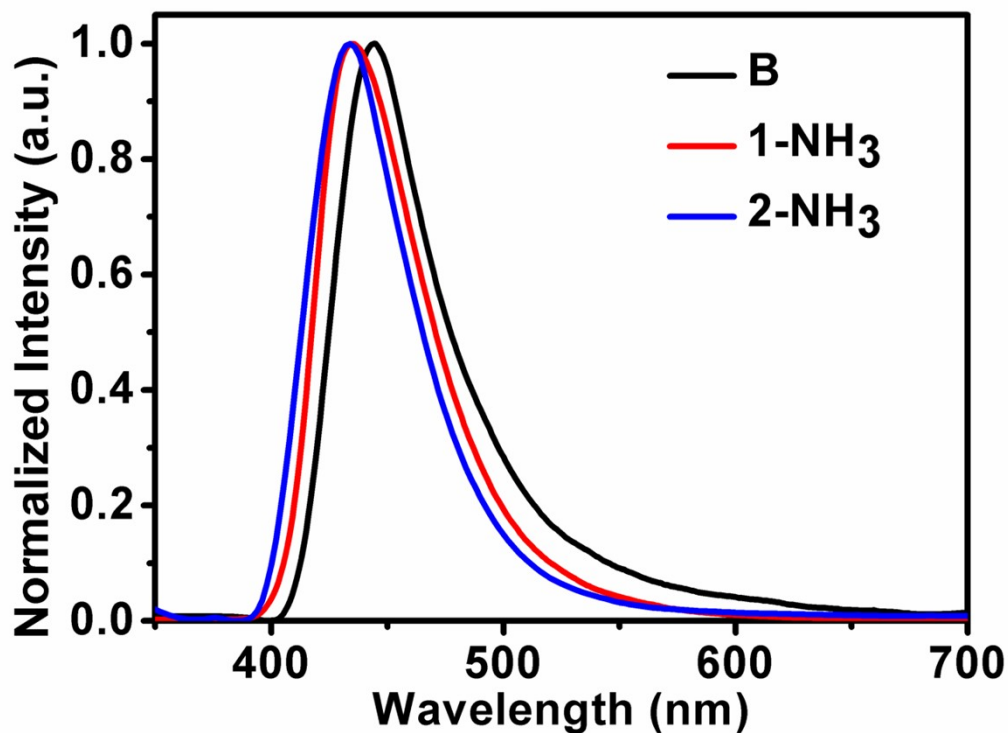


Figure S4. Fluorescence emission spectra of **B**, **1-NH₃** and **2-NH₃**.

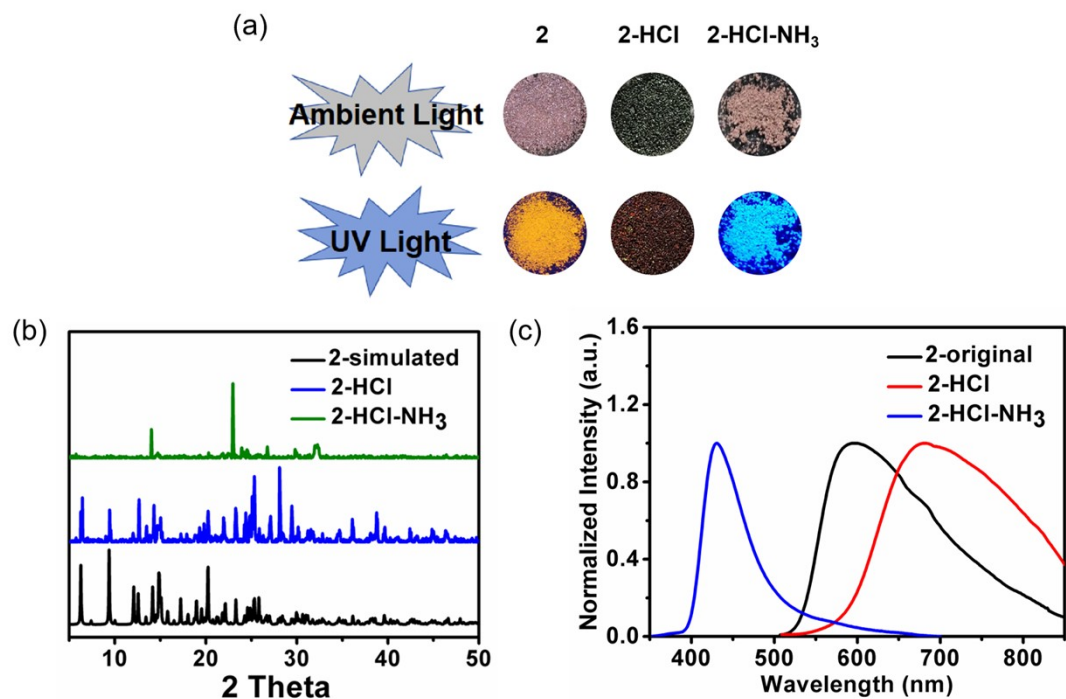


Figure S5. (a) Photographs under ambient light and 365 nm UV light. (b) PXRD patterns. (c) Fluorescence emission spectra of complex **2** and the samples exposed to HCl/NH₃ vapor. (d) Thermogravimetric curves of complex **2** before and after fumigation by HCl vapor.

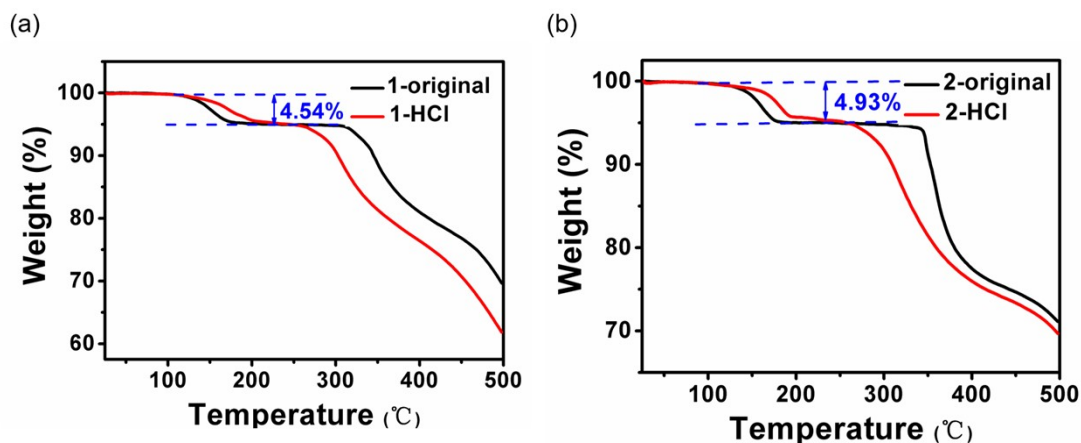


Figure S6. Thermogravimetric curves of complex **1** (a) and complex **2** (b) before and after fumigation by HCl vapor.

Comparison of the fluorescence of complex **1** and the Schiff base ligand

The optimized molecular configurations and frontier orbitals (HOMO and LUMO) were shown in **Figure S7**. It can be seen that the HOMO and LUMO of complex **1** are mainly located in the ligand.

I⁻ and Zn²⁺ ions did not contribute to the frontier orbitals. The LUMO of complex **1** is similar to that of Schiff base. While the HOMO of complex **1** is a little different from that of the Schiff base. It is located in the whole molecule of the Schiff base. Thus the fluorescence of complex **1** is mainly affected by the Schiff base ligand, but different from the Schiff base. **Figure S8** shows the distortion angle between the pyridine and benzene planes is -172.80 and -175.07° in complex **1** and the Schiff base ligand, respectively, which indicates the Schiff base has better coplanarity in the absence of Zn(II) ion. Thus the emission peak of the Schiff base ligand may red shift compared with that of complex **1**.

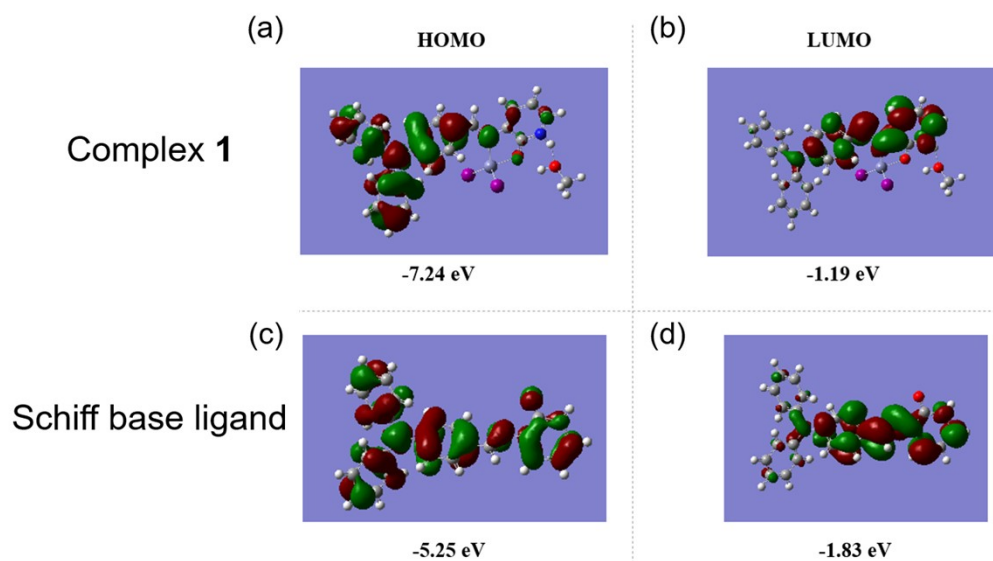


Figure S7 The optimized molecular configurations and orbitals (HOMO and LUMO) of complex **1** and Schiff base ligand.

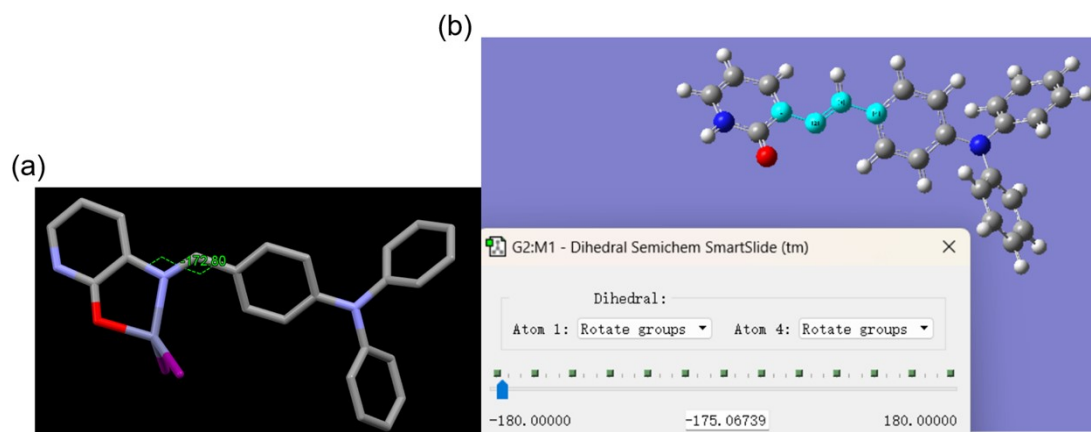


Figure S8 Molecular structure of complex **1** (a) and Schiff base ligand (b) showing the distortion angle between the pyridine and benzene planes.

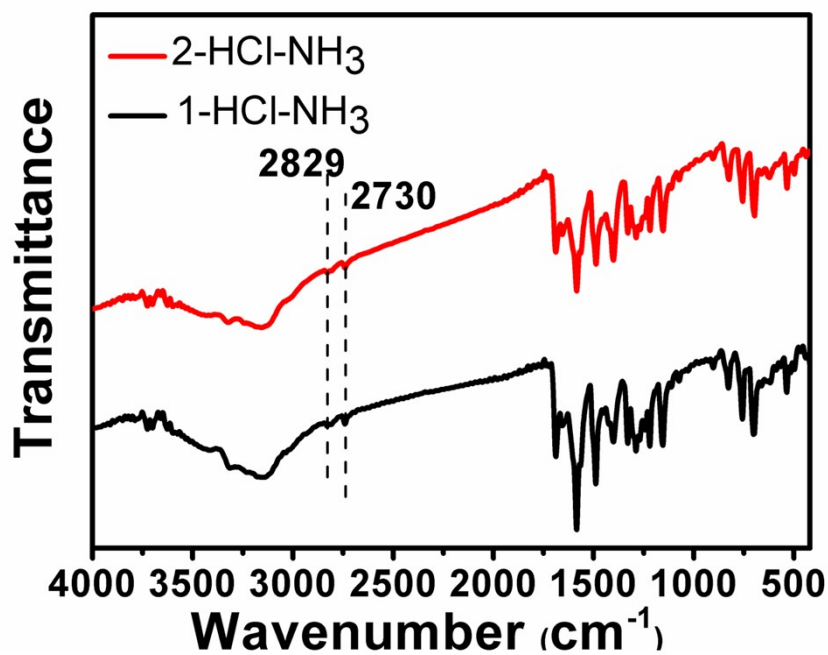


Figure S9. IR spectra of 1-HCl-NH₃ and 2-HCl-NH₃.

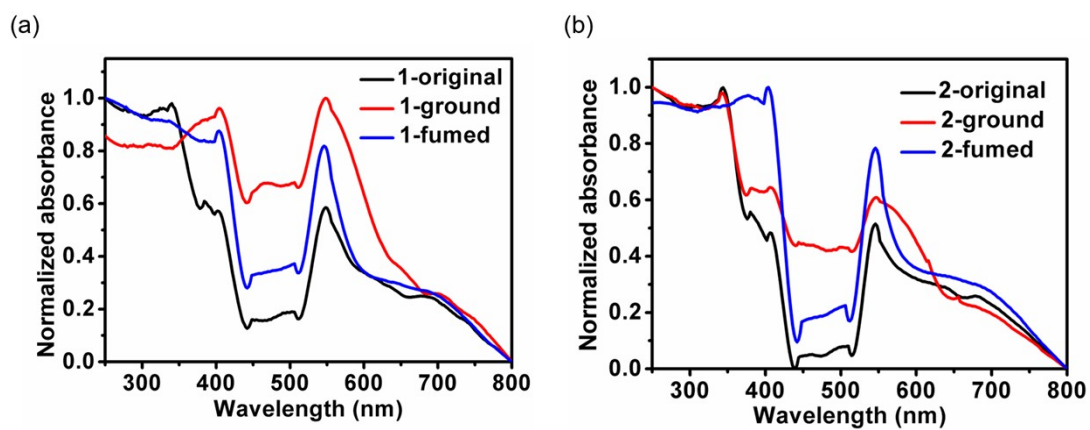


Figure S10. UV-vis absorption spectra of complexes 1 (a) and 2 (b) before and after grinding and fumed.

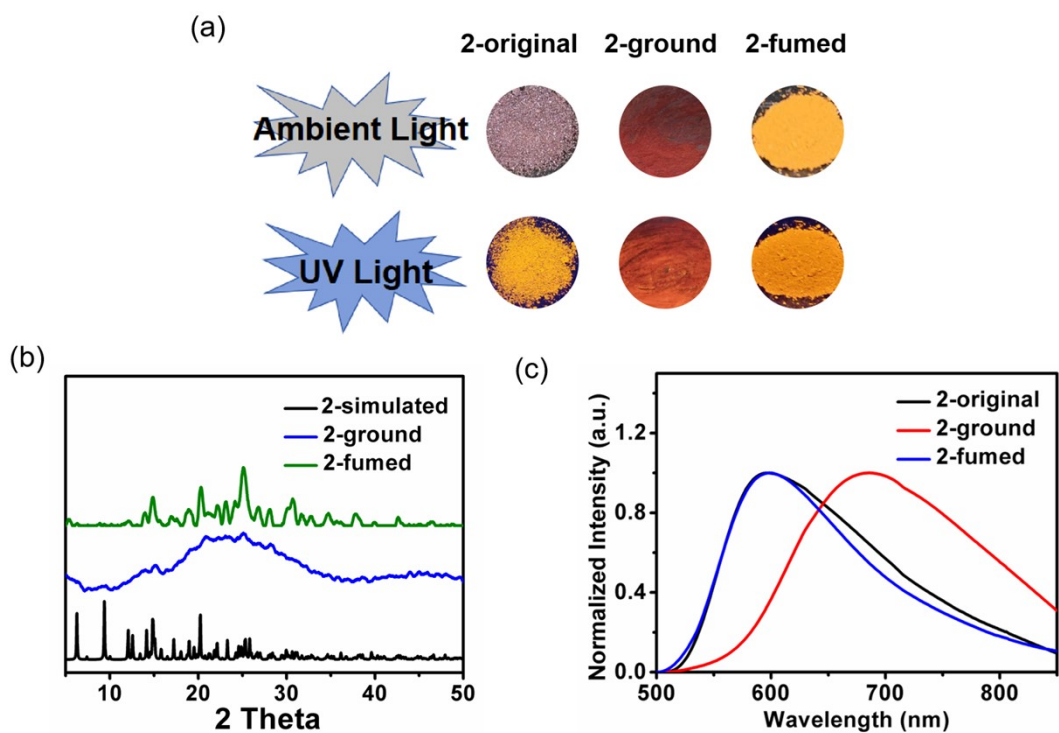


Figure S11. (a) Photographs under ambient light and 365 nm UV light. (b) PXRD patterns. (c) Fluorescence emission spectra of the original crystals of complex **2** before and after grinding and fumed.

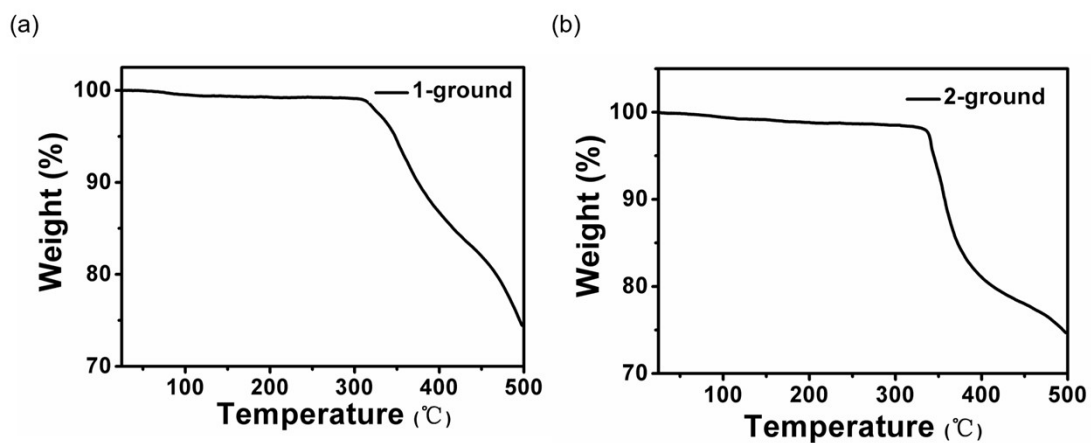


Figure S12. Thermogravimetric curves of complex **1** (a) and complex **2** (b) after grinding.

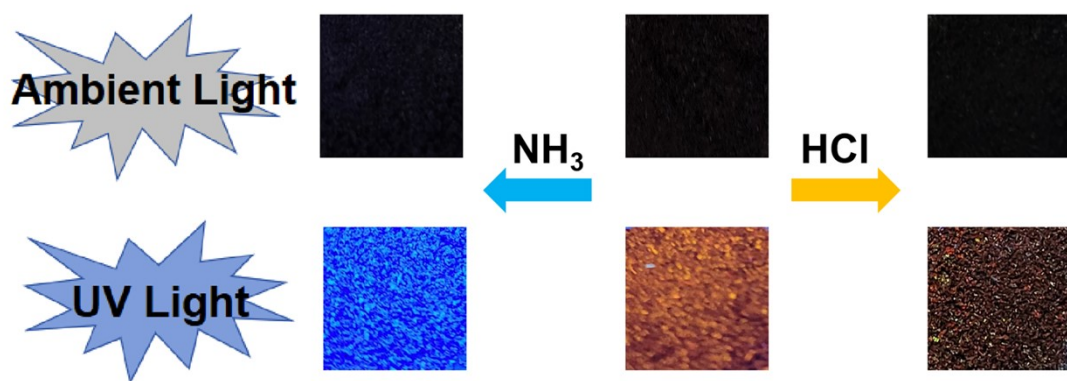


Figure S13. Photographs of the complex **2** test paper after different treatments under natural light and 365 nm irradiation.

Table S1 Crystal data and structure refinement parameters of complexes **1** and **2**.

Complex	1	2
Empirical formula	C ₂₅ H ₂₃ I ₂ N ₃ O ₂ Zn	C ₂₅ H ₂₃ Br ₂ N ₃ O ₂ Zn
Formula weight	716.63	622.65
Temperature/K	100.01(10)	100.01(10)
Crystal system	Triclinic	Triclinic
Space group	P $\bar{1}$	P $\bar{1}$
a/Å	7.5135(2)	7.3928(3)
b/Å	12.1526(6)	11.9818(4)
c/Å	14.5092(4)	14.0657(4)
α /°	92.374(3)	93.806(3)
β /°	99.647(2)	99.114(3)
γ /°	96.671(3)	95.971(3)
Volume/Å ³	1294.73(8)	1219.17(7)
Z	2	2
ρ_{calc} /cm ³	1.838	1.696
μ /mm ⁻¹	3.359	4.312
F(000)	692.0	620.0
Radiation	Mo K α (λ = 0.71073)	Mo K α (λ = 0.71073)
Goodness-of-fit on F ²	1.041	1.062
Final R indexes [$I \geq 2\sigma(I)$]	R ₁ = 0.0337, wR ₂ = 0.0688	R ₁ = 0.0390, wR ₂ = 0.0948
Largest diff. peak/hole / e Å ⁻³	0.76/-0.68	1.20/-0.89
CCDC number	2250683	2254633

Table S2. Selected bond distances (Å) and angles (°) for **1** and **2**.

Complex 1			
I1—Zn3	2.5490(4)	I2—Zn3	2.5526(4)
Zn3—O4	2.002(2)	Zn3—N5	2.086(3)
I1—Zn3—I2	117.139(14)	O4—Zn3—I1	113.69(7)
O4—Zn3—I2	109.24(7)	O4—Zn3—N5	83.55(10)
N5—Zn3—I1	113.38(8)	N5—Zn3—I2	115.09(7)

Complex 2			
Br1—Zn3	2.3563(5)	Br2—Zn3	2.3584(5)
Zn3—N24	2.076(2)	Zn3—O31	2.002(2)
Br1—Zn3—Br2	117.925(18)	N24—Zn3—Br1	112.48(7)
N24—Zn3—Br2	115.13(7)	O31—Zn3—Br2	109.04(6)
O31—Zn3—Br2	109.04(6)	O31—Zn3—N24	83.29(9)

Table S3. The photophysical data of complex **1** in different states.

The state of complex 1	Fluorescence emission
Original	614 nm
1-NH ₃	435 nm
1-NH ₃ -HCl	429 nm
1-HCl	720 nm
1-HCl-NH ₃	433 nm
Ground	712 nm
Fumed	610 nm

Table S4. The photophysical data of complex **2** in different states.

The state of complex 2	Fluorescence emission
Original	600 nm
2-NH ₃	427 nm
2-NH ₃ -HCl	430 nm
2-HCl	683 nm
2-HCl-NH ₃	431 nm
Ground	688 nm
Fumed	600 nm

Table S5. The fluorescence lifetime $\langle\tau\rangle$ of **1** and **2**.

complex	τ_1 (ns)	A_1 (%)	τ_2 (ns)	A_2 (%)	$\langle\tau\rangle$ (ns)	χ^2
1	0.8960	95.69	0.1200	4.31	0.86	1.293
2	1.1831	97.48	0.1500	2.52	1.16	1.140